

Pseudorotation in Water Trimer Isotopomers Using Terahertz Laser Spectroscopy

Mark R. Viant, Jeff D. Cruzan,[†] Don D. Lucas,[‡] Mac G. Brown, Kun Liu,[§] and Richard J. Saykally*

Department of Chemistry, University of California, Berkeley, California 94720

Received: March 3, 1997; In Final Form: May 23, 1997[⊗]

We report the first observation of five water trimer isotopomers using terahertz laser spectroscopy coupled with a pulsed slit jet expansion technique. A single c-type vibration–rotation–tunneling (VRT) band has been observed for each isotopomer between 40 and 50 cm^{-1} . By considering all the experimental data, including results from isotopic substitution experiments, analyses of bifurcation tunneling splittings, and rotational analyses of the VRT bands, it has been possible to determine unambiguously the isotopic composition and structure of each isotopomer. We have also extended the measurements of the 41.1 cm^{-1} band in $(\text{D}_2\text{O})_3$, first reported by Suzuki and Blake [Suzuki, S.; Blake, G. A. *Chem. Phys. Lett.* **1994**, 229, 499]. All six VRT bands have been assigned to pseudorotational transitions, which principally involve flipping of the “free” hydrogen or deuterium atoms in the trimer from above to below the plane of the OOO ring. Interestingly, four of the six bands have been assigned to the same transition. The four trimers responsible for these bands, designated d_6 , d_5a , d_4a , and d_3a , form a series in which the three deuterium atoms in the ring are sequentially substituted by hydrogen atoms. The corresponding experimental band origins for d_6 to d_3a show a 1–2 cm^{-1} blue shift upon each substitution. Existing pseudorotation models are unable to satisfactorily account for this result. We propose that, if the hydrogen or deuterium atoms within the ring are allowed to participate in the flipping motion, this band origin shift can be explained.

I. Introduction

There has been much recent activity in the study of water clusters, both experimentally^{1–14} and theoretically,^{15–32} with the ultimate goal of advancing the detailed molecular description of liquid water. The development of far-infrared vibration–rotation–tunneling (FIR VRT) spectroscopy has allowed the first high-resolution observation of the water trimer,^{2–8} tetramer,^{9,10} pentamer,^{11,12} and most recently, the water hexamer.¹³ This technique has proven to be a powerful tool for accessing both structural and dynamical information. Theoretical studies of water clusters have been ongoing for many years, with particular emphasis on the smaller clusters. This work has focused on the calculation of ab initio potential energy surfaces, optimized structures, and transition states,^{15–21} the effect of three-body interactions,^{22,23} and analysis of the hydrogen-bond network rearrangement (HBNR) pathways^{24–26} occurring in these clusters. However, recent experimental work on the larger water clusters is currently stimulating many such studies of these species as well.

The water trimer was first studied in 1982 by Y. T. Lee and co-workers, using infrared vibrational predissociation spectroscopy.³³ Over 10 years later, Pugliano and Saykally reported a rotationally resolved (and strongly perturbed) spectrum of $(\text{D}_2\text{O})_3$ using far-IR VRT spectroscopy.² They determined the structure to be a cyclic ring, with each water monomer acting as single donor and single acceptor of a hydrogen bond, in agreement with ab initio calculations.^{15,16} The equilibrium structure is shown in Figure 1, with the three H (or D) atoms in the OOO plane termed “bound”, and the three H (or D) atoms

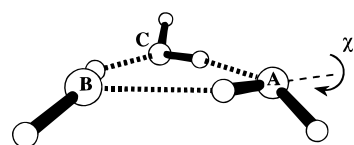


Figure 1. The ab initio equilibrium structure (C_1 symmetry) of the water trimer, showing the location of the oxygen atoms (A, B, and C) and the bound and free H or D atoms. Also indicated is one of the three internal rotation angles ($\chi_A = 57.3^\circ$, $\chi_B = 50.9^\circ$, $\chi_C = -61.6^\circ$)¹⁷ associated with the flipping motion of the free H or D atoms.

sticking out of the ring termed “free”; note that the equilibrium structure is asymmetric with C_1 symmetry. More recently, Liu et al.³ reported the observation of an exact oblate top spectrum for the water trimer. This is now understood to result from one type of dynamical behavior exhibited by the trimer, the facile flipping of the free H (or D) atoms from above to below the OOO plane. This flipping motion has been the subject of much theoretical work in which it is described in terms of a pseudorotation model.^{27–30} Calculations have been reported using one-, two-, and three-dimensional (1-D, 2-D, and 3-D) models, but the most sophisticated treatment is by van der Avoird and co-workers,³⁰ which in addition to three internal torsional coordinates includes overall rotation of the trimer. This attention has resulted from the contention that all seven VRT bands reported for pure water trimer result from pseudorotational transitions. Although much progress has been made in modeling the experimental data, even the most sophisticated theory and the most recent torsional potential energy surfaces require further refinement, as demonstrated in this paper.

For the water trimer, the focus of both the experimental and theoretical work has so far been on the isotopically pure species, $(\text{H}_2\text{O})_3$ and $(\text{D}_2\text{O})_3$. Very recently, however, the isotopically substituted trimers have been considered; the only theoretical studies to date are the pseudorotation calculations by van der Avoird and co-workers³⁰ and by Leutwyler and co-workers,³⁴ as well as a diffusion Monte Carlo study by Clary and co-workers.³⁵ Although the latter two papers focus exclusively

[†] Present address: Department of Molecular and Cellular Biology, Harvard University, Cambridge, MA 02138.

[‡] Present address: Department of Earth, Atmospheric and Planetary Sciences, Massachusetts Institute of Technology, Cambridge, MA 02139.

[§] Present address: Department of Chemistry, University of Southern California, University Park, Los Angeles, CA 90089.

* To whom correspondence should be addressed.

[⊗] Abstract published in *Advance ACS Abstracts*, October 1, 1997.

on isotopically substituted water trimers, neither study explicitly considers the isotopomers studied in the present work. The introduction of hydrogen into $(D_2O)_3$ or deuterium into $(H_2O)_3$ lowers the symmetry of the cluster and changes the observed tunneling fine structure patterns, rotational constants, and vibrational band origins. Consequently, these species are a stringent test for the models of pseudorotation and tunneling dynamics and for the quality of trial potential energy surfaces. The only previous experimental work on water trimer isotopomers is by Liu et al.,⁶ who reported the observation of two bands; their analysis focused on the $(D_2O)_2(HDO)$ trimer with the H atom occupying a free position. This paper described in some detail the permutation inversion (PI) group theory necessary to explain the bifurcation tunneling patterns that were observed. Bifurcation tunneling (or “donor tunneling”) involves a single H_2O (or D_2O) monomer in the trimer switching its bound and free H (or D) atoms. Much theoretical work has addressed this important tunneling pathway as well.^{24–26}

This paper reports the observation and analyses of five isotopically substituted water trimer VRT bands close to 40 cm^{-1} , all of which are believed to result from pseudorotational transitions. Three of these bands exhibit bifurcation tunneling, and the group theoretical treatment reported by Liu et al.⁶ is used to explain the observed splittings. The emphasis of this paper is on the analysis of the pseudorotational frequencies, using the best available theoretical models, to gain further insight into this complicated vibrational motion; improvements in the model for both pure and isotopically substituted trimers are suggested. We have also extended the measurements of the pure $(D_2O)_3$ band at 41.1 cm^{-1} that was first reported by Suzuki and Blake.⁵

It is important to clarify the nomenclature used in this paper. Each unique water trimer *structure* has a label, for example d_5a , where the “ d_5 ” describes the number of deuterium atoms within the cluster, and the “ a ” differentiates this particular species from another (“ b ”) containing five D atoms. A total of nine unique trimer structures will be considered here; d_6 , d_5a , d_5b , d_4a , d_4b , d_3a , d_3b , h_5a , and h_6 . An additional numeral is sometimes added to the structure label, for example $d_5a(I)$, where the “ I ” labels the observed transition. Hence, if an equivalent transition is observed in two different water trimer species, the resulting *bands* are labeled $d_5a(I)$ and $d_4a(I)$. Finally, a hydrogen bond involving an H atom will be called just that, while one involving a D atom will be termed a deuterium bond.

II. Experimental Section

The Berkeley terahertz laser spectrometers have been described in detail elsewhere,³⁶ and hence only the principal features and recent changes to the experiment will be presented here. Tunable far-infrared (FIR) light is generated by nonlinear mixing of two independent sources of radiation in a Schottky barrier diode. A high power (100 W), line tunable, infrared CO_2 laser coaxially pumps a fixed frequency, molecular gas far-IR laser, the output of which is coupled through free space onto the diode. Two far-IR lasers were used for the work described here, 1299.9954 GHz (CH_3OD) and 1397.1186 GHz (CH_2F_2). The fundamental, first- or second-harmonic from a HP8673B microwave (MW) synthesizer ($2–26\text{ GHz}$) is coupled onto the diode giving a continuous frequency coverage of $2–60\text{ GHz}$. The mixing of the fixed frequency far-IR radiation with the tunable MW radiation in the diode produces tunable sidebands at frequencies $\nu_{FIR} \pm n\nu_{MW}$. The sidebands are multipassed 14–22 times through a molecular beam expansion before impinging on an InSb hot electron bolometer. The multipass cell, consisting of two spherical mirrors, is arranged in the Herriott configuration.³⁷

The slit valve assembly used to produce the pulsed molecular beam expansion has been described in detail previously.³⁸ The carrier gas, either pure Ar, 70% Ne in He, or pure He, is first bubbled through a mixture of water before being expanded through a 101.6 mm long slit. For the work presented here a series of water mixtures were used containing different mole fractions of D_2O relative to H_2O . Nozzle backing pressures in the range 1–2 atm were employed, the actual value being dependent on the carrier gas. At a pulse rate of 43 Hz the vacuum chamber was maintained at a pressure of approximately 40 mTorr (for Ar carrier gas) by a 1200 l s^{-1} mechanical booster (Edwards EH4200) backed by two rotary pumps (Edwards E2M275).

Transient absorption signals measured on the InSb bolometer are modulated at both the repetition rate of the slit valve (43 Hz) and at the modulation frequency of the far-IR radiation (50 kHz). The timing of the slit valve is controlled by a pulse generator (Stanford Research Systems DG535). Following preamplification, the transient signal is band-pass filtered (SRS SR560 low-noise preamplifier). A lock-in amplifier (SRS SR810) demodulates the frequency modulation of the far-IR radiation using $2f$ detection at 100 kHz and a $100\text{ }\mu\text{s}$ time constant. The signal is then collected by a digital storage oscilloscope (Tektronix TDS320) which typically averages 32 pulses of the slit valve. The resulting averaged absorption profile is downloaded and integrated by a 486-PC to yield a single data point. The advantage of this method over boxcar integration is that we now collect the entire absorption signal (typically 2 ms wide), whereas the maximum gate width of a typical boxcar is less than $500\text{ }\mu\text{s}$. An active background subtraction method is employed whereby two 1 ms sections of the averaged waveform, one on each side of the absorption signal, are themselves averaged to yield a base line, which is then subtracted from the waveform. Although Doppler limited line widths (fwhm) of 0.9 MHz were obtained, the frequency uncertainty of each line is 3 MHz, arising from the uncertainty in the output frequency of the far-IR laser.

III. Results and Analysis

We report the observation and assignment of five new VRT bands obtained by expanding carefully controlled mixtures of D_2O and H_2O through a pulsed slit. All the observed bands are c-type (parallel), and yield spectra similar in appearance to the 41.1 cm^{-1} VRT band in $(D_2O)_3$, first observed by Suzuki and Blake.⁵ Furthermore, all five bands lie within 5 cm^{-1} of this pure trimer band. As a result of using a pulsed slit expansion we have approximately doubled the number of transitions observed in the 41.1 cm^{-1} band as compared to the original study. In fact, the strongest lines in this band have been recorded with a signal-to-noise ratio of 2600 to 1.

For a mixed D_2O and H_2O expansion, determining the exact cluster species responsible for a given spectral line required a series of investigations since no explicit mass selectivity is employed in our experiments. First, isotope substitution experiments were undertaken to determine the ratio of D to H within a given cluster. Second, the observation of tunneling splittings in the spectra, which require the exchange of equivalent nuclei, helped determine whether the monomers constituting the trimer were H_2O , D_2O , or HDO. Finally, the complete analysis of the spectra to yield rotational constants and vibrational band origins was necessary to determine whether a particular H or D atom was located within the ring or was free. The following sections describe each of these methods in more detail. Furthermore, the spectra were recorded using pure Ar and pure He as the expansion gas, thus eliminating the possibility that the clusters contained carrier gas atoms.

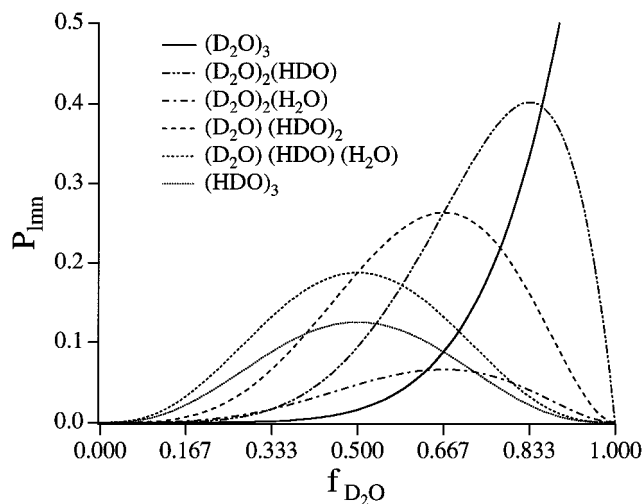


Figure 2. A plot of the probability (P_{lmm}) of forming various trimer isotopomers ($(\text{D}_2\text{O})_l(\text{HDO})_m(\text{H}_2\text{O})_n$) as a function of the mole fraction of D_2O in the mixed $\text{H}_2\text{O}/\text{D}_2\text{O}$ expansion. For clarity, only trimers containing at least three D atoms are included. Note that a given trimer isotopomer abundance is maximized when $f_{\text{D}_2\text{O}}$ equals the ratio of the number of D atoms in the cluster, divided by 6.

Isotope Substitution Experiments. Varying the isotopic composition of the water expanded through the slit changes the relative abundances of the various water cluster isotopomers formed in the supersonic expansion. Consequently, by characterizing the intensity of a particular spectral line as a function of isotopic composition of the water, the ratio of D to H in the molecular carrier of the line can be determined unambiguously. Relative abundances of clusters formed in the expansion are expected to depend not only on statistics, but also on energetics. A hydrogen bond in the trimer is approximately 50 cm^{-1} less stable than a deuterium bond,³⁵ and hence it is energetically preferable for a D atom to occupy a ring position than to be free. However, considering only the statistics of cluster formation, the probability of forming a cluster $(\text{D}_2\text{O})_l(\text{HDO})_m(\text{H}_2\text{O})_n$ is given by

$$P_{lmm} = 2^m \sigma_{lmm} (f_{\text{D}_2\text{O}})^{2l+m} (1 - f_{\text{D}_2\text{O}})^{m+2n} \quad (1)$$

where

$$\sigma_{lmm} = \frac{(l+m+n)!}{(l!m!n!)} \quad (2)$$

and $f_{\text{D}_2\text{O}} = (1 - f_{\text{H}_2\text{O}})$ is the mole fraction of D_2O in the water mixture. Here we are interested in the water trimer, for which $l+m+n=3$. Figure 2 shows a plot of the probability of formation of various trimer isotopomers as a function of $f_{\text{D}_2\text{O}}$. The D_2O mole fraction which maximizes a given isotopomer is equal-to-the ratio of the number of D atoms in the trimer to the total number of D and H atoms. For example, a $(\text{D}_2\text{O})_2(\text{HDO})$ signal maximizes at $f_{\text{D}_2\text{O}} = 5/6$. Again, this is neglecting kinetic isotope effects. Experimentally, a strong Q-branch transition from each spectrum was recorded at $f_{\text{D}_2\text{O}}$ equal to $5/6$, $4/6$, $3/6$, and $2/6$. The mixture at which a given transition maximized identified the spectral carrier. This is shown in Figure 3 for three of the observed bands, allowing an unambiguous assignment of the carriers to the d_{5a} , d_{4a} , and d_{3a} trimers. The same method was used to assign the carriers of the two remaining bands to the d_{4b} and d_{3b} trimers.

Although eq 1 correctly predicts the D_2O mole fraction at which a given cluster size is maximized, the situation becomes more complicated when trying to determine the abundance of

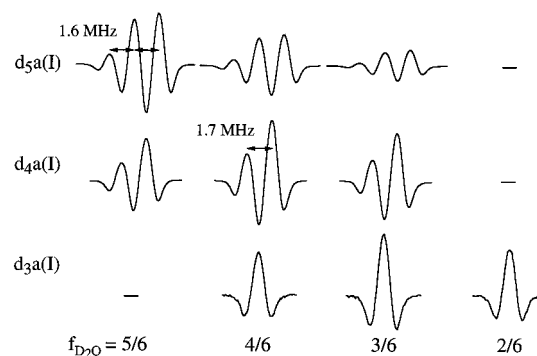


Figure 3. Experimental VRT spectra of a single Q-branch transition from each of the $d_{5a}(\text{I})$, $d_{4a}(\text{I})$, and $d_{3a}(\text{I})$ bands, recorded at four different mole fractions of D_2O ($f_{\text{D}_2\text{O}} = 5/6, 4/6, 3/6,$ and $2/6$) expanded through the slit jet. The set of three spectra corresponding to each particular trimer are plotted on the same vertical scale. From the value of $f_{\text{D}_2\text{O}}$ which maximizes a given signal we can determine the isotopic composition of that trimer, e.g., the spectra corresponding to the d_{4a} trimer maximizes at $f_{\text{D}_2\text{O}} = 4/6$, confirming the presence of four D atoms in that cluster. The bifurcation tunneling splittings in the $d_{5a}(\text{I})$ and $d_{4a}(\text{I})$ bands are also shown.

each unique structure in which the positions of all the H and D atoms are specified. For example, by varying the H and D atoms between bound and free positions there are 2^3 possible structures for $(\text{HDO})_3$, some of which are equivalent. In fact four unique structures exist, having either three, two, one, or no H atoms in the free positions. Consequently, the abundance of any one of these structures is only some fraction of the probability P_{030} . This allows an interesting comparison to be made: if the abundance of $(\text{D}_2\text{O})_3$ is defined as 1.0 (using an optimized expansion with $f_{\text{D}_2\text{O}} = 1.0$), then the abundance of $(\text{HDO})_3$ with all D atoms free is only 0.0156 (using an optimized expansion with $f_{\text{D}_2\text{O}} = 0.5$). Hence, even under optimized conditions, the number density of $(\text{HDO})_3$ in the molecular beam should be approximately 64 times smaller than that for $(\text{D}_2\text{O})_3$. This illustrates an inherent disadvantage associated with measuring the spectra of trimer isotopomers. To compare intensities between different isotopomer spectra, the nuclear spin statistics of the levels involved in a transition need to be considered in addition to the statistics of cluster formation.

Tunneling Splittings. The observation of tunneling splittings in far-IR VRT spectroscopy directly yields information on the internal dynamics of water clusters. One of the most important tunneling pathways in the water trimer is bifurcation tunneling,^{24–26} which exchanges the bound and free H(D) atoms on a particular water monomer within the cluster. In the pure water trimer, this results in every rovibrational line splitting into a quartet pattern.^{3,30} The spacings of the individual lines in the quartet are typically 1–5 MHz for $(\text{D}_2\text{O})_3$ and 250–300 MHz for $(\text{H}_2\text{O})_3$, the larger splitting corresponding to the faster tunneling motion of the lighter H atoms. An observable splitting generally results only if the monomer undergoing the tunneling is H_2O or D_2O ; for HDO the exchange of the H and D atoms is a nondegenerate process. Consequently, the observation of any tunneling patterns from isotopically substituted water trimers can help identify the carrier of the VRT band.

Bifurcation tunneling in water trimer isotopomers is discussed in detail by Liu et al.⁶ They focused their analysis on a $(\text{D}_2\text{O})_2(\text{HDO})$ trimer, which contains two monomers capable of undergoing bifurcation tunneling. However, the presence of the HDO monomer forces the two D_2O monomers to be inequivalent, one being a donor and one an acceptor to the HDO. This results in an unequally spaced quartet tunneling pattern. However, it was shown that if this inequivalence was small then the two central peaks of the quartet would become accidentally

degenerate, and a triplet tunneling pattern would result. They used this argument to explain the observed triplet patterns associated with the $K_c'' = K_c' = 0$ transitions of their $(D_2O)_2$ - (HDO) band. The $(D_2O)(HDO)_2$ and $(H_2O)(HDO)_2$ trimers present a simpler situation, wherein only a single monomer is able to undergo bifurcation tunneling. This results in a doublet tunneling pattern.⁶

The five new isotopically substituted trimer bands presented here can be divided into three categories. The $d_{3a}(I)$ and $d_{3b}(III)$ bands did not exhibit any tunneling splittings, the $d_{4a}(I)$ and $d_{4b}(II)$ bands contained doublet patterns, and the $d_{5a}(I)$ band showed a triplet tunneling pattern (see Table 1). Furthermore, experimental spectra of the $d_{5a}(I)$, $d_{4a}(I)$, and $d_{3a}(I)$ tunneling patterns are shown in Figure 3. The absence of any tunneling splittings implies the absence of any H_2O and D_2O monomers within the cluster. Thus the d_{3a} and d_{3b} trimers must have an isotopic composition of $(HDO)_3$, with an indeterminate arrangement of H and D atoms (using just the tunneling data). The 1.7 and 2.6 MHz doublet splittings in the $d_{4a}(I)$ and $d_{4b}(II)$ bands, respectively, imply the presence of a single homogeneous monomer, and hence two HDO monomers, in each cluster. Comparison of the magnitude of these splittings with those for pure $(H_2O)_3$ and $(D_2O)_3$ very strongly suggests that the single homogeneous monomer must be D_2O . Consequently the isotopic composition of the d_{4a} and d_{4b} trimers is almost certainly $(D_2O)(HDO)_2$. As well as considering the splitting pattern and spacings, the intensities of the peaks can be related directly to nuclear spin statistical weights. For $(D_2O)(HDO)_2$ the predicted doublet should have a 1:2 intensity ratio,⁶ as observed experimentally for both the $d_{4a}(I)$ (see Figure 3) and $d_{4b}(II)$ bands. Finally, the $d_{5a}(I)$ band exhibits a triplet tunneling pattern, with a spacing between the individual lines of 1.6 MHz, consistent with the cluster containing two homogeneous monomers and hence one HDO monomer. Again, the magnitude of the splitting strongly suggests that $(D_2O)_2(HDO)$ is the isotopic composition of the d_{5a} trimer. As confirmation, the predicted intensity pattern⁶ for this trimer from nuclear spin weights is 1:4:4, as observed experimentally and shown in Figure 3.

Analysis of Spectra. A recording of the $5_{15} \leftarrow 5_{05}$ Q-branch transition in the d_{4a} trimer is shown in Figure 4 (a), and a stick spectrum of the entire c-type $d_{4a}(I)$ trimer band is shown in Figure 4 (b). Four of the isotopomer VRT bands exhibit asymmetry doubling and hence were fit to an asymmetric rotor Hamiltonian, while the fifth isotopomer band as well as the remeasured $(D_2O)_3$ band, denoted $d_6(I)$, were fit to an oblate symmetric top Hamiltonian. Since the observed spectra were c-type (or parallel) for near oblate (or perfect oblate) top molecules, and hence all transitions obey $\Delta K_c = 0$, only the difference between the ground and excited-state C rotational constants could be determined. In the fitting procedure C'' (ground state) for each band was fixed at a value close to $(A'' + B'')/4$, the case for a perfect planar top, while C' (excited state) was varied.

Table 1 includes the number of lines observed in each band, the results of the fits and a summary of the observed tunneling splittings. For comparison, spectroscopic constants for the 87.1 cm^{-1} pure $(H_2O)_3$ band,³ denoted $h_6(I)$, and the isotopically substituted $(D_2O)_2(HDO)$ cluster band⁶ in which the H atom is free, denoted $d_{5b}(IV)$, are also included in the Table. A number of points can be highlighted concerning the five new isotopomer VRT bands. First, all bands are completely unperturbed and are individually fit to a semirigid rotor expression with rms errors of residuals of less than 1 MHz. Second, the rotational constants of the five new species lie between those values for pure $(D_2O)_3$ and $(H_2O)_3$, strongly suggesting that the bands result

TABLE 1: Optimized Spectroscopic Parameters from the Least-Squares Fits of Eight VRT Bands of Pure and Isotopically Substituted Water Trimer Species^a

trimer	$d_6(I)$	$d_{5a}(I)$	$d_{4a}(I)$	$d_{5a}(I)$	$d_{4b}(II)$	$d_{3b}(III)$	$d_{5b}(IV)^b$	$h_6(I)^c$
A''	5796.58 (4)	5907.99 (10)	5955.72 (4)	5940.98 (4)	6426.23 (8)	6478.67 (7)	6195.69 (29)	6646.94 (2)
B''	$=A''$	5783.11 (10)	5832.12 (4)	$=A''$	6047.48 (8)	6099.85 (7)	5833.90 (25)	$=A''$
D_J''	0.0344 (6)	0.0283 (29)	0.0338 (5)	0.0323 (7)	0.0363 (fixed)	0.0363 (15)	0.1350 (fixed)	0.0414 (1)
D_{JK}''	-0.0521 (14)	-0.0464 (51)	-0.0484 (13)	-0.0497 (16)	-0.0505 (fixed)	-0.0505 (40)	6192.48 (28)	-0.0619 (6)
A'	5792.97 (5)	5902.04 (7)	5948.53 (5)	5934.16 (4)	6422.81 (8)	6463.54 (7)	5811.80 (29)	6626.16 (2)
B'	$=A'$	5779.49 (7)	5827.33 (5)	$=A'$	6031.71 (8)	6095.05 (7)	$=A'$	$=A'$
D_J'	0.0281 (6)	0.0257 (17)	0.0276 (5)	0.0278 (8)	0.0379 (3)	0.0384 (16)	0.1358 (3)	0.0400 (2)
D_{JK}'	-0.0458 (15)	-0.0441 (40)	-0.0421 (13)	-0.0451 (18)	-0.0520 (3)	-0.0526 (41)	-7.871 (51)	-0.0604 (6)
ΔC	11.86 (2)	11.75 (2)	11.84 (1)	12.01 (2)	-4.42 (1)	-4.03 (2)	2.917 820.44 (87)	0.82 (1)
band origin	1 232 140.33 (34)	1 283 478.64 (25)	1 329 895.03 (23)	1 372 214.54 (34)	1 392 426.06 (25)	1 375 644.45 (25)	2 609 774.63 (20)	
lines in fit	87	66	115	64	57	50		
rms error	1.15	0.773	0.990	0.853	0.804	0.535		
tunneling pattern	quartet	triplet	doublet	singlet	doublet	singlet	triplet and quartet	quartet
trimer formula	$(D_2O)_3$	$(D_2O)_2(HDO)$	$(D_2O)(HDO)_2$	$(HDO)_3$	$(D_2O)(HDO)_2$	$(HDO)_3$	$(D_2O)_2(HDO)$	$(H_2O)_3$

^a Parameters listed in column $d_6(I)$ result from an extended analysis of the 41.1 cm^{-1} band (transition frequencies and assignments are available from the authors on request), first observed by Suzuki and Blake (ref 5). The $d_{5a}(I)$, $d_{4a}(I)$, $d_{4b}(II)$, and $d_{3b}(III)$ bands were recorded and analyzed in the present study (transition frequencies are available from the author on request) while the $d_{5b}(IV)$ (ref 6) and $h_6(I)$ (ref 3) bands were observed previously. All values are in units of MHz, and numbers in parentheses are one standard deviation. Also tabulated are the bifurcation tunneling patterns of a single rovibrational transition for each band, and the trimer formulas deduced from the isotope substitution experiments, tunneling patterns, and spectral analyses. ^b Reference 6. ^c Reference 3.

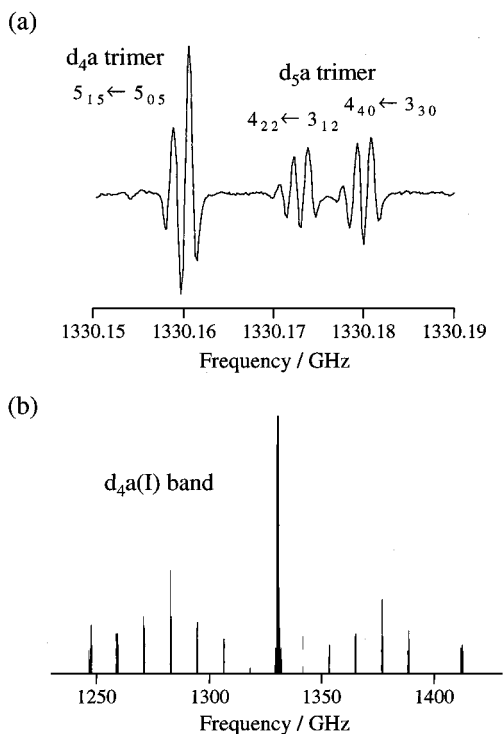


Figure 4. (a) A typical experimental VRT spectrum showing the characteristic bifurcation tunneling patterns of the d_{4a} trimer (1:2 doublet) and d_{5a} trimer (1:4:4 triplet). Note that the overlap of the bands has placed a d_{4a} Q(5) transition adjacent to d_{5a} R(3) transitions. (b) A stick spectrum of the c-type $d_{4a(I)}$ trimer band showing all observed lines.

from trimer clusters; a detailed analysis of the rotational constants is presented below.

By collating the conclusions from the isotope experiments, the observed tunneling splittings and analyses of the bands we can deduce the isotopic compositions of the clusters responsible for the five VRT bands; they are listed in the bottom row of Table 1. The final step is to determine the actual structures, viz. for each HDO monomer is the D atom bound or free. Although the experimental rotational constants are contaminated by the dynamics, they still contain sufficient structural information to allow this to be done.

Analysis of Rotational Constants. If the water trimer were semirigid, locating the H and D atoms in an isotopomer using Kraitchman's equations³⁹ and a sufficient data set of rotational constants would be possible. However the trimer exhibits a high degree of nonrigidity, in particular, the facile flipping of the free H or D atoms from above to below the plane of the OOO ring. Calculations based upon the equilibrium structure, in which two H(D) atoms lie above the ring and one H(D) atom lies below, are clearly unsuitable as this gives rise to an asymmetric top molecule which is not found experimentally for the pure trimers. A better choice would be to average the free H(D) atoms into the plane of the OOO ring; however, rather small and unrealistic R(O—O) separations are then required to reproduce the rotational constants for the pure trimers. It has been shown from an analysis of the most probable flipping angle associated with the flipping dynamics⁶ that a free H(D) atom spends approximately half of the time localized at some angle above the OOO plane and half at the same angle below the plane. Therefore, although physically unrealistic, this suggests that the following geometrical model could account for the vibrational averaging, and hence reproduce the rotational constants. All six atoms within the ring are treated as "normal", but every free atom of mass m is treated as two "half-atoms",

TABLE 2: Comparison of the Rotational Constants Predicted for Nine Isotopically Substituted Trimer Species with the Experimental Values^a

water trimer formula	predicted constants/MHz		experimental data/MHz		assignment
	A''_{pred}	B''_{pred}	A''	B''	
(D ₂ O) ₂ (HDO)					
H bound	5914	5796	5908	5783	d_{5a}
H free	6166	5843	6196	5834	d_{5b}
(D ₂ O)(HDO) ₂					
2 H bound	5971	5855	5956	5832	d_{4a}
1 H bound, 1 H free	6273	5860			
2 H free	6388	6054	6426	6047	d_{4b}
(HDO) ₃					
3 H bound	5971	$= A''_{\text{pred}}$	5941	$= A''$	d_{3a}
2 H bound, 1 H free	6280	5972			
1 H bound, 2 H free	6445	6123	6479	6100	d_{3b}
3 H free	6445	$= A''_{\text{pred}}$			

^a Comparison allows an unambiguous structural characterization of the d_{5a} , d_{4a} , d_{3a} , d_{4b} , and d_{3b} trimers, and confirmation of the structure of the previously reported d_{3b} trimer (ref 6). Note that the d_{3a} trimer yields a perfect symmetric top spectrum as predicted by the theory.

each of mass $m/2$, one lying at some angle above the OOO plane and the other at the same angle below; the calculation of rotational constants for the trimer isotopomers presented here is based on this model.

In the calculation, the geometries of the monomers³¹ within the trimer were fixed throughout, with equilibrium bound and free O—H(D) bond lengths of 0.9572 Å and a bond angle of 104.5°. The equilibrium values were used because for the accuracy required here, the zero-point and equilibrium values are almost identical. The oxygen atoms were assumed to lie at the corners of an equilateral triangle with an R(O—O) separation of 2.840 Å, as determined in a recent Monte Carlo calculation which was fit to experimental data.⁶ The three bound H(D) atoms were assumed to occupy vibrationally averaged positions in the OOO plane, forming O—H(D)···O bond angles of 148°; this is a reasonable approximation as in the equilibrium structure the bound H(D) atoms are predicted to lie, on average, only 5.5° out of the OOO plane.²³ Finally, the six "half-atoms" were assumed to lie at some angle θ both above and below the OOO plane. The first step in the calculation involved optimizing this angle θ to match the rotational constants derived from this model structure to the experimental values for (D₂O)₃.³ A result of $\theta = 61^\circ$ was obtained, reasonably consistent with the value of 50° from the Monte Carlo calculations by Liu et al.⁶ Having determined the optimum structure from a fit to (D₂O)₃ data, rotational constants for (H₂O)₃ were calculated. The difference between the predicted and experimental values of B'' was only 15 MHz which confirmed, considering the level of this calculation, that holding the geometry of the cluster fixed during isotopic substitution of D atoms by H atoms was reasonable. A more detailed discussion on geometry changes accompanying isotopic substitution is presented below.

It has been concluded previously that the five new VRT bands result from transitions in (D₂O)₂(HDO), (D₂O)(HDO)₂ and (HDO)₃ trimers. Hence the A'' and B'' rotational constants for all nine possible trimer structures with these formulas were calculated, and the results are presented in Table 2. Also shown in this table are the A'' and B'' constants derived from the rotational analyses of the five new bands and the constants from the only previously analyzed trimer isotopomer band.⁶ A comparison of the predicted and experimental data allows an unambiguous assignment of the carrier of each VRT band. The discrepancy between the predicted and experimental A'' and B'' rotational constants for the six assigned bands is on average 21

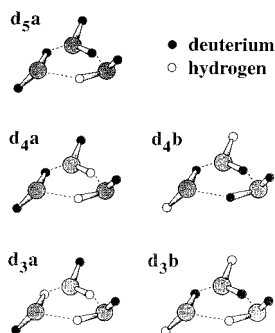


Figure 5. The equilibrium structures of the five observed water trimer isotopomers, d_{5a} , d_{4a} , d_{3a} , d_{4b} , and d_{3b} . Note that the d_{4b} and d_{3b} trimers, both with two H atoms free, have been arbitrarily depicted with one H atom above, and one below, the plane of the ring.

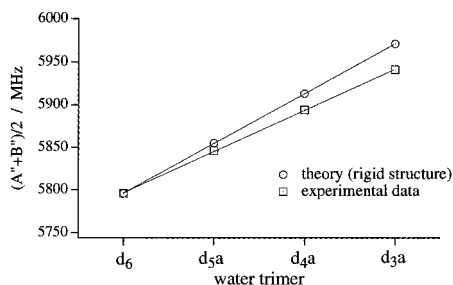


Figure 6. A plot of the average ground-state rotational constants, $(A'' + B'')/2$, for the trimers d_6 , d_{5a} , d_{4a} , and d_{3a} . Both the experimental and theoretical values were fit to straight lines yielding correlation coefficients of 0.9999. The rigid model structure used to obtain the theoretical values was optimized for $(D_2O)_3$, explaining the agreement between experiment and theory for this trimer.

MHz and at worst less than 40 MHz (<1%). Figure 5 shows the *equilibrium structures* of the five observed isotopomers; for the d_{4b} and d_{3b} trimers, both with two H atoms free, the structures have been arbitrarily depicted with one H atom above, and one below, the OOO plane.

Previous experimental work on the pure water trimer³ has shown that by rapid vibrational averaging of the hydrogen bond torsional coordinates a perfect oblate top spectrum is obtained, even though the equilibrium structure is asymmetric (C_1 symmetry). However, even after considering these flipping dynamics, the structures of the d_{5a} , d_{4a} , d_{4b} , and d_{3b} isotopomers remain asymmetric. Consequently the spectra obtained should all exhibit asymmetry doubling, as was indeed observed experimentally. Furthermore, vibrational averaging of the d_{3a} trimer does generate a perfect oblate top and hence no asymmetry doubling is expected, which is exactly what was observed.

Having determined the structures of the observed trimer species, an interesting progression becomes apparent. The four trimers, d_6 , d_{5a} , d_{4a} , and d_{3a} , all have three D atoms free, and progression along this series involves the stepwise substitution of the three bound D atoms by H atoms. Figure 6 shows both the experimental ground-state rotational constants and the rotational constants obtained from our rigid model structure calculation, plotted against the degree of isotopic substitution; since the d_{5a} and d_{4a} trimers are asymmetric rotors the average of the A'' and B'' constants have been plotted. The two sets of data were fit to straight lines, and correlation coefficients of 0.9999 were obtained for both. This result allows us to draw some interesting conclusions regarding the structural rearrangement of the trimer skeleton upon isotopic substitution. Because the zero-point energy associated with a hydrogen bond is larger than that of a deuterium bond, the hydrogen bond is expected to be slightly longer. The theoretical rotational constants plotted

in Figure 6, which lie in a near perfect straight line, were obtained from the model structure with no structural rearrangement included. Calculations were also undertaken which included an effective lengthening of the R(O—O) separation upon substitution of a D atom by a H atom. These plots did not yield straight lines through all four data points. In fact, the greater the increase of the R(O—O) separation upon substitution, the greater the deviation of the plot from linearity. Since the experimental data has been shown to lie in a near perfect straight line we can conclude that the change in the R(O—O) separation, from the d_6 through to the d_{3a} trimer is very small; this is in agreement with the Monte Carlo calculations by Liu et al.⁶ This conclusion is further supported by considering the d_{3a} trimer, which contains three hydrogen bonds. Figure 6 shows that the experimental A'' constant is 30 MHz smaller than the predicted value obtained from the model structure with no structural rearrangement; it is important to remember that this model structure was optimized for pure $(D_2O)_3$, which obviously contains three deuterium bonds. Holding all parameters in the model structure fixed, except for the R(O—O) separation, this 30 MHz discrepancy can be accounted for by lengthening the R(O—O) separation in the hydrogen bonded trimer to 2.848 Å, an increase of only 0.008 Å.

IV. Vibrational Analysis

Including the $d_6(I)$ band, there are a total of six pure and isotopically substituted trimer VRT bands lying within a 5 cm^{-1} region. An obvious question arises: has the same vibrational transition been observed in each of the six different trimer species, with the shift in the band origins resulting from the effect of isotopic substitution? To answer this, the origin of the known $d_6(I)$ trimer band at 41.1 cm^{-1} must be ascertained.

The $(D_2O)_3$ trimer consists of three monomers, each of which can undergo a low frequency torsional vibration. This torsional motion involves the flipping of a free D atom from above to below (and vice versa) the OOO plane, through a low potential barrier. However, the constraints imposed by the symmetry of the potential energy surface of the trimer cause the flipping of the three D atoms to couple together. The resultant sequential flipping motion is termed pseudorotation because it is indistinguishable from a c -axis inertial rotation of the entire cluster. Several theoretical studies of pseudorotation in the water trimer, from 1-D,²⁷ 2-D²⁸, and 3-D²⁹ calculations, up to a very recent and sophisticated calculation which also includes overall rotation of the cluster³⁰ have been reported. The potential barrier to this motion is calculated to lie below the 3-D zero-point energy (ZPE) levels for $(D_2O)_3$ and $(H_2O)_3$,^{24,32} and consequently this motion produces very large (many wavenumbers) "tunneling splittings" or, as it has been referred to, a pseudorotational energy level manifold. This manifold can be accordingly considered to result from low frequency torsional modes of the cluster.

Most calculations assign the 41.1 cm^{-1} band in $(D_2O)_3$ to a pseudorotational transition from the ground-state $k = 0$ ($1a_g$ symmetry) to the lower $|k| = 3$ ($1a_u^{\text{lower}}$ symmetry) level,^{28–30} where k is the pseudorotation quantum number and the symmetry labels are obtained from the $C_{3h}(M)$ molecular symmetry group; here we label the $k = 0 \rightarrow |k| = 3^{\text{lower}}$ transition as transition I. The Hamiltonian for internal motion, developed by van der Avoird and co-workers,³⁰ is used to calculate pseudorotational eigenvalues and is comprised of four terms:

$$H_{\text{internal}} = -\frac{\hbar^2}{8\pi^2} \sum_{\nu} \frac{\partial^2}{\Lambda_{\nu} \partial \chi_{\nu}^2} + \frac{1}{2} A (j_{+}^{\dagger} j_{+} + j_{-}^{\dagger} j_{-}) + C j_z^{\dagger} j_z + V(\chi_A, \chi_B, \chi_C) \quad (3)$$

The first term is the internal rotation kinetic energy operator, and depends on both the effective internal rotational constant, $F^{\text{eff}} = \hbar^2/8\pi^2\Lambda_{\nu}$, for the constrained monomer rotation, and the internal rotation angle χ_{ν} (see Figure 1), where the summation is over the three monomers (labeled by ν). The second and third terms (Coriolis terms), containing the components of j , arise because the rotations of the free H(D) atoms are expressed with respect to the moving trimer frame.³⁰ The fourth term describes the torsional potential energy surface (PES) for the water trimer, and depends principally on the internal rotation angle χ_{ν} for each monomer in the cluster. Two analytical torsional PESs have been reported in the literature, both extracted from ab initio calculations.^{31,32}

Starting with the Hamiltonian for $(\text{D}_2\text{O})_3$, and determining the effect of isotopic substitution on the terms in this Hamiltonian, we can deduce vibrational shifts for different trimer species. First, within the Born–Oppenheimer approximation, the torsional potential energy surface is insensitive to isotopic substitution of the D atoms by H atoms, so this term is considered constant. The contribution of the second and third terms in the Hamiltonian to transition I in $(\text{D}_2\text{O})_3$ (at 41.1 cm^{-1}) is calculated to be either 0.85 cm^{-1} (2.1%) or 1.09 cm^{-1} (2.7%) depending upon which torsional PES was used.³⁰ These two terms depend on the trimer rotational constants which, from Table 1, increase by up to about 10% in going from pure $(\text{D}_2\text{O})_3$ to the five isotopically substituted trimers under discussion. Consequently, not only is the contribution of the second and third terms in eq 3 small, but it varies very little between the pure and isotopically substituted trimers, allowing us to ignore it here. The term in the Hamiltonian which is most sensitive to isotopic substitution is the internal rotation kinetic energy, depending explicitly on the effective internal rotational constant of each constrained monomer.

Two methods have previously been used to determine effective internal rotational constants for the constrained water monomers;^{30,40} from ref 30, $F_{\text{D}_2\text{O}}^{\text{eff}}$ has been calculated to equal 11.73 cm^{-1} and $F_{\text{H}_2\text{O}}^{\text{eff}}$ to equal 21.39 cm^{-1} . These values were calculated using geometries for isolated water monomers, neglecting the small r_{OH} lengthening that occurs on hydrogen bond formation. The ratio of these constants gives an approximate scaling factor between the pseudorotational energy level manifolds for $(\text{D}_2\text{O})_3$ and $(\text{H}_2\text{O})_3$, assuming χ_{ν} to be the same for D_2O and H_2O monomers. Consequently, transition I at 41.1 cm^{-1} in $(\text{D}_2\text{O})_3$ is predicted to occur at about twice this frequency for $(\text{H}_2\text{O})_3$. As shown in Table 1, a band at 87.1 cm^{-1} has been observed³ in $(\text{H}_2\text{O})_3$ and has been assigned to transition I.³⁰ This shows that complete isotopic substitution of $(\text{D}_2\text{O})_3$ by H atoms causes a large band origin shift of almost 50 cm^{-1} .

Using an expression from ref 30, and monomer geometries from ref 31 the effective internal rotational constants for the constrained HDO monomer can be calculated. For the case of the D atom occupying a free position within the trimer structure, $F_{\text{HDO}}^{\text{eff}}$ (D free) = 11.73 cm^{-1} , and for the H atom free, $F_{\text{HDO}}^{\text{eff}}$ (H free) = 21.39 cm^{-1} . These values are the same, to 4 significant figures, as those for the constrained D_2O and H_2O monomers, respectively. This result is actually not so surprising when one inspects the model used to calculate F^{eff} . The monomers are constrained to internal rotation about an axis which passes through the monomer center of mass and the bound H(D) atom.

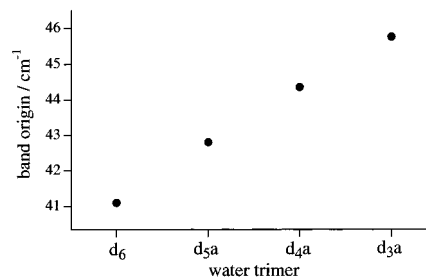


Figure 7. A plot of the observed VRT band origins, for transition I, in the d_6 , d_{5a} , d_{4a} , and d_{3a} trimers. Upon sequential replacement of the three bound D atoms by H atoms the band origins are blue-shifted by 1.71, 1.55, and 1.41 cm^{-1} , respectively.

Consequently, the bound H(D) atom is assumed to be fixed and plays no role in the determination of the effective internal rotational constant.

Under the constraints of this model, the validity of which will be discussed below, interesting conclusions concerning pseudorotational transition frequencies in trimer isotopomers can be ascertained. First, consider the $(\text{HDO})_3$ trimer with all three H atoms free: the internal rotation kinetic energy operator for this species will be the same as for $(\text{H}_2\text{O})_3$, and hence the transition frequencies for these trimers will be essentially the same. Similarly, the $(\text{HDO})_3$ trimer with all three D atoms free will share the same pseudorotational energy level manifold as $(\text{D}_2\text{O})_3$, as, in fact, would all trimers which have three free D atoms. Here we are assuming that any coupling between the three internal rotation kinetic energy operators is the same for a trimer isotopomer as it is for the pure species. The d_6 , d_{5a} , d_{4a} , and d_{3a} trimers all have three D atoms free, and therefore the same transition in all four trimers should occur at essentially the same frequency. Experimentally the four observed VRT bands all lie within only 5 cm^{-1} of each other (near 41 cm^{-1}). Although there is some disagreement between the theoretical prediction and experimental data, which is discussed below, this model calculation suggests the bands do indeed all result from the same pseudorotational transition (transition I).

Figure 7 shows a plot of the experimental VRT band origins as a function of the degree of isotopic substitution. Upon sequential replacement of D atoms by H atoms in the three bound positions in the trimer ring, the band origins are blue-shifted by 1.71, 1.55, and 1.41 cm^{-1} , respectively. This unexpected result is significant, with the total $d_6(\text{I})$ to $d_{3a}(\text{I})$ shift of 4.67 cm^{-1} greater than 10% of the original $(\text{D}_2\text{O})_3$ transition frequency. At first we attempted to explain this shift within the constraints of the existing model by allowing only the free D atoms to move during the vibration. The frequency associated with this flipping depends, to some degree, on the mass of the entire trimer. This can be modeled using a second method for calculating effective internal rotational constants, discussed in ref 40; here the principal moments of inertia for the trimer, which clearly depend on the extent of isotopic substitution, feature explicitly in the determination of F^{eff} . The calculations were undertaken using the transition structure for the flipping motion (with a free D atom in the OOO plane), and taking the internal rotation axis to lie along the appropriate bound O–H(D) bond. The values obtained for F^{eff} were 9.938 cm^{-1} for d_6 and 9.944 cm^{-1} for d_{3a} . The ratio of these constants can be used to estimate the theoretical vibrational shift going from the 41.1 cm^{-1} band in d_6 to the equivalent band in d_{3a} . The model correctly predicts that a blue-shift should be observed, but with a magnitude of only 0.024 cm^{-1} , which is clearly not compatible with the experimental observation.

A second possible origin for the 4.67 cm^{-1} experimental blue-shift arises from the distortion of the monomer geometry on

forming the trimer (monomer “relaxation”). Schütz et al.²⁷ reported *ab initio* values for the free and bound O–H bond lengths of 0.959 Å and 0.970–0.971 Å, respectively. Compared to using the isolated monomer equilibrium geometry in the calculation, the elongation of the bound O–H bond causes the monomer center of mass to shift and hence changes the effective internal rotational constant. Using the method in ref 30 the new F^{eff} values obtained are 12.182 cm^{-1} for d_6 and 12.261 cm^{-1} for d_{3a} . Once again the effect correctly predicts a blue-shift for the $d_6(\text{I})$ to $d_{3a}(\text{I})$ bands, but from the ratio of the above constants, with a magnitude of only 0.27 cm^{-1} .

We propose that to account for the 4.67 cm^{-1} experimental shift the *bound* H(D) atoms must also be included in the vibrational motion. In this case the substitution of a lighter H atom for a bound D atom which is directly participating in the motion will lead to a much larger increase in the transition frequency. The question arises as to what extent do the bound H(D) atoms contribute in the vibration. We know that the blue shift in going from $d_6(\text{I})$ to $d_{3a}(\text{I})$ is 4.67 cm^{-1} . The additional blue-shift in going from $d_{3a}(\text{I})$ to $h_6(\text{I})$ is 41.28 cm^{-1} . Clearly, the extent to which the bound H(D) atoms contribute is small compared to the free H(D) atoms, but it is still far from negligible.

This explicit involvement of bound H(D) atoms in the torsional motion has never been considered in any of the calculations on pseudorotation in water trimer.^{27–30} In the model employed by Leutwyler and co-workers²⁹ torsional motion (or internal rotation) of each monomer is constrained to occur about an axis passing through the oxygen atom and the bound H(D) atom. In the model used by van der Avoird and co-workers,³⁰ the same motion is constrained to an axis passing through the center of mass of the monomer and the bound H(D) atom. Therefore, in both models the bound H(D) atoms were fixed to simplify the calculations. In support of our conclusions, the $(\text{D}_2\text{O})_3$ normal-mode analysis of Schütz and co-workers²⁷ does predict the involvement of the bound H(D) atoms in the low frequency torsional vibrations.

It is interesting to speculate on the way in which the bound H(D) atoms are involved in the vibrational motion. The simplest modification to the original model would involve retaining a single internal rotation axis for each flipping monomer, but for each of these three axes to be moved slightly, such that they no longer pass through the bound H(D) atoms. Unless the three water monomers are strongly coupled by the potential energy surface, each will prefer to internally rotate about an inertial axis passing through the monomer center of mass. Hence, to demonstrate the importance of involving the bound H(D) atoms, we chose new internal rotation axes that connect the center of masses of adjacent monomers. This corresponds to each axis lying close to the OOO plane at an angle of approximately 20° inside of the bound O–H(D) bonds. Using this revised model the effective internal rotational constants for the constrained water monomers were calculated as follows:³⁰ $F_{\text{D}_2\text{O}}^{\text{eff}} = 13.86 \text{ cm}^{-1}$, $F_{\text{HDO}}^{\text{eff}}$ (D free) = 14.44 cm^{-1} , $F_{\text{HDO}}^{\text{eff}}$ (H free) = 23.04 cm^{-1} , and $F_{\text{H}_2\text{O}}^{\text{eff}} = 25.36 \text{ cm}^{-1}$. Using these values in eq 3 the theory correctly predicts, at least qualitatively, that a pseudorotational transition in the d_{3a} trimer will occur at higher frequency than in the d_6 trimer. Quantitatively, an approximate blue-shift can be obtained from the ratio of the effective internal rotational constants. The equivalent transition to the 41.1 cm^{-1} band in d_6 is now predicted to occur at 42.8 cm^{-1} in d_{3a} ; the measured d_{3a} band origin is 45.8 cm^{-1} . This confirms that changing the locations of the internal rotation axes changes both the vibrational band origins and the corresponding frequency shifts. However, the predicted band origin shift from d_6 to d_{3a} only

accounts for approximately 40% of the observed shift. In reality it is very probable the torsional motion is more complicated, with no single fixed internal rotation axis able to describe the motion of each flipping monomer.

We have also observed two other trimer isotopomers, d_{4b} and d_{3b} , both having a single D atom and two H atoms free. From the above discussion, if transition I were to occur in these trimers we would expect the band origins to lie many wavenumbers higher than the observed values of 46.4 and 45.9 cm^{-1} . This is in agreement with the recent work by Leutwyler and co-workers,³⁴ who predict the equivalent transition to that at 41.1 cm^{-1} in $(\text{D}_2\text{O})_3$ to occur at 56.9 cm^{-1} in $(\text{H}_2\text{O})_2(\text{D}_2\text{O})$; note that their paper predicts the $(\text{H}_2\text{O})_2(\text{D}_2\text{O})$, d_{4b} and d_{3b} trimers, all with one D atom and two H atoms free, to have equivalent pseudorotational manifolds “to within a very good approximation”. This strongly suggests that the $d_{4b}(\text{II})$ and $d_{3b}(\text{III})$ bands do not originate from transition I, but the question again arises, do they both result from the same transition? For the d_6 to d_{3a} trimer series (transition I), replacing a single bound D atom by an H atom causes a 1–2 cm^{-1} blue shift of the band origin which, at least qualitatively, can be explained. Assuming the $d_{4b}(\text{II})$ and $d_{3b}(\text{III})$ bands both originate from the same transition, the equivalent substitution from the d_{4b} to d_{3b} trimer causes a red shift of 0.56 cm^{-1} . Since this is contrary to our previous observation, it appears unlikely, to a first approximation, that these bands originate from the same transition and are appropriately labeled $d_{4b}(\text{II})$ and $d_{3b}(\text{III})$.

The $d_{4b}(\text{II})$ and $d_{3b}(\text{III})$ bands probably result from pseudorotational transitions; first, from Table 1, the values of ΔA , ΔB , and ΔC for these and the other pure and isotopically substituted trimer bands, are small. This is consistent with a vibrational mode involving only light atom motion, such as torsion of the free H and D atoms. Furthermore, before the pseudorotation model was developed, *ab initio* calculations²⁷ predicted the lowest frequency intermolecular mode in $(\text{H}_2\text{O})_3$ to occur at 111.4 cm^{-1} . Just as pseudorotation in pure water trimer is necessary to account for the high number of observed low-frequency (<100 cm^{-1}) VRT bands, so it can account for the low-frequency 46.4 and 45.9 cm^{-1} $d_{4b}(\text{II})$ and $d_{3b}(\text{III})$ trimer bands, respectively.

A reasonable assignment for these transitions can be obtained from the recent 3-D pseudorotation calculation on water trimer isotopomers.³⁴ Approximating the d_{4b} and d_{3b} trimers to have a pseudorotational manifold equivalent to the $(\text{H}_2\text{O})_2(\text{D}_2\text{O})$ trimer, the most likely assignment for both bands is the c -type $n = 1$ (a^-) to $n = 4$ (a^+) transition, where n is a level number. This transition is predicted at 44.5 cm^{-1} , less than 2 cm^{-1} from the experimental band origins. Consistent with this assignment is the fact that both bands are relatively weak (maximum signal-to-noise ratio of 30:1), as would be expected for transitions originating from the first excited state of the pseudorotational manifold. This assignment of the $d_{4b}(\text{II})$ and $d_{3b}(\text{III})$ bands to the same transition is, however, contrary to our earlier conclusion. This discrepancy could perhaps be explained by considering other dynamical effects, such as coupling between the internal rotation kinetic energy operators or coupling of the three torsional modes with other modes. These effects might shift the lower and upper states in the $n = 1$ to $n = 4$ transitions in both the isotopomers by different amounts, which could yield nonintuitive ordering of the band origins. Clearly more work must be undertaken to fully characterize pseudorotation in water trimer isotopomers.

V. Discussion

Nondegenerate tunneling, occurring between potential minima associated with different structures and energies, differs from

degenerate tunneling in that it does not ordinarily lead to spectroscopically observable splittings. Consequently its occurrence is difficult to recognize in a spectrum. For the isotopomers reported here, each HDO monomer could be undergoing nondegenerate bifurcation tunneling. However, a deuterium bond in the trimer is approximately 50 cm^{-1} more stable than a hydrogen bond.³⁵ Consequently the probability for such tunneling is small. This suggests that the orientation of each HDO monomer in a trimer is frozen from the moment of formation in the free jet expansion. The experimental data are entirely consistent with this hypothesis as can be seen from Table 2, which includes the ground state rotational constants for six isotopically substituted trimer species. The structures of d_5a and d_5b differ only in the location of the single H atom. If nondegenerate bifurcation tunneling was occurring on a rapid time scale, these two structures would become indistinguishable. From Table 2, however, it is evident that d_5a and d_5b have different rotational constants and hence different structures. Thus on the time scale of our experiment we can deduce that nondegenerate bifurcation tunneling is not occurring. Referring to Table 2 and Figure 5, a similar argument exists on the basis of the comparison of the structures of d_4a and d_4b , and d_3a and d_3b . Furthermore, the spectra of the trimers containing just HDO monomers show no evidence for splittings or line broadening compared to pure $(D_2O)_3$.

For the series of trimers from d_6 to d_3a (transition I), the energetic stability of each cluster decreases as deuterium bonds are replaced by hydrogen bonds. We have observed this particular series simply as a result of our spectrometer scanning between 40 and 48 cm^{-1} . Our results do not suggest that the abundances of these isotopomers are greater than for trimers containing deuterium bonds, which are more stable. Another trimer series should exist from h_6 to h_3 (also transition I), where bound H atoms are stepwise substituted by D atoms, thus forming increasingly stable clusters. The first isotopomer of this series, h_5a , with a single D atom bound, has been observed experimentally;⁶ the $h_5a(I)$ band origin is red-shifted from the 87.1 cm^{-1} $h_6(I)$ band by approximately 1 cm^{-1} . This observation is exactly as expected and serves to strengthen our hypothesis that bound H(D) atoms are explicitly involved in the torsional motions of the water trimer.

Much theoretical work on pseudorotation in pure water trimers has been reported,^{27–29} the most sophisticated by van der Avoird and co-workers.³⁰ However, discrepancies still exist between the experimental VRT band origins^{2–5,7,8} and those values predicted by theory; for example, the 41.1 cm^{-1} band observed in $(D_2O)_3$ is predicted to occur at either 24.7 or 36.6 cm^{-1} depending upon which effective torsional PES is used in the calculation.³⁰ To reproduce the experimental data accurately relies on the development of both a realistic dynamical model and an accurate potential surface. Two ideas are proposed below to explain these discrepancies in light of the present work on the isotopically substituted water trimer species.

One of the principal conclusions from this work is the suggested involvement of the bound H(D) atoms in the torsional vibrations of water trimer. This has not been considered in any of the previous theoretical models of pseudorotation dynamics. In the last section we showed that by arbitrarily shifting the internal rotation axes of the water monomers, such that the axes no longer pass through the bound H(D) atoms, the trend in VRT band origins for the d_6 to d_3a trimer series (transition I) could be reproduced, at least qualitatively. With regard to the pure water trimer, the shifting of these axes will change F^{eff} , the effective internal rotational constant for constrained monomer rotation. Since this constant features explicitly in the Hamil-

tonian for internal motion, eq 3, this will also cause the energy of each eigenfunction in the pseudorotational manifold to change.

A second source of discrepancy between the theoretical and experimental pseudorotational transition frequencies depends upon the effective torsional PES. The complete PES for the water trimer, assuming the monomer geometries are held rigid, is twelve dimensional. To extract a torsional PES from the complete 12-D surface, 9 coordinates must be fixed and a 3-D “cut” taken which depends only on the 3 torsional angles. i.e. the six-membered hydrogen-bonded ring is held rigid. For the torsional PESs calculated by the van Duijneveldts³¹ and by Bürgi et al.,³² these three angles describe rotation of each constrained monomer about an axis passing through the oxygen atom and the bound H(D) atom. From the present work we have shown this is not the correct position for the internal rotation axes, and hence the wrong 3-D “cut” has been taken through the 12-D PES. This confirms the suggestion by the van Duijneveldts who stated, “Moreover, it is not likely that the bending will precisely be along the H-bonded OH as rotation axis. Actual calculations of the VRT spectra using both available potentials are needed to bring forward those features of the model that need to be improved”.³¹ Using an improved and more realistic torsional PES would change the energy levels in the pseudorotational manifold, which should then yield theoretical transition frequencies more similar to the experimental values.

Finally we consider how the involvement of the bound H(D) atoms in the torsional motion might affect the zero-point inertial defect of the water trimer; this quantity, defined as $\Delta = I_c^0 - I_b^0 - I_a^0$, gives an indication of the planarity of a molecule and the nature of the vibrational motion. From experimentally derived rotational constants for the lower state of the 98.1 cm^{-1} band,³ which is thought to be the ground state, the inertial defect for $(D_2O)_3$ is -10.75 amu \AA^2 . This large negative value is characteristic of out-of-plane motions, viz., the rapid out-of-plane flipping motions of the free D atoms. The Monte Carlo simulation of these torsional vibrations by Liu et al.⁶ calculated an inertial defect of -5.90 amu \AA^2 . They commented that since out-of-plane motions contribute negatively to Δ , the discrepancy between the theoretical and experimental values could be explained by other out-of-plane motions neglected in their model. This suggestion is consistent with the conclusions from the present work, since the participation of the bound H(D) atoms in the torsional vibration, which they neglected, will cause these atoms to move out of the OOO plane and hence lower the inertial defect.

VI. Conclusions

We have reported the observation of a single VRT band in each of five previously unobserved water trimer isotopomers, and have extended the measurements of a $(D_2O)_3$ band first observed by Suzuki and Blake.⁵ A complete analysis of the experimental data, including isotope substitution results, tunneling splittings and rotational constants, was performed to unambiguously assign a specific trimer structure to the carrier of each VRT band. From the ground-state rotational constants for the d_6 to d_3a trimer series, it was concluded that the R(O—O) separation undergoes minimal change upon isotopic substitution. This result is in agreement with the Monte Carlo calculations of Liu et al.⁶

Using the most sophisticated pseudorotation theory by van der Avoird and co-workers,³⁰ we have suggested that the $d_6(I)$, $d_5a(I)$, $d_4a(I)$, and $d_3a(I)$ bands all result from the same pseudorotational transition in each of the four trimers. Although the theoretical predictions and experimental results are to some

degree consistent, a large enough discrepancy remains to warrant a refinement of the theory. We suggest that the 4.67 cm^{-1} blue shift from the $d_6(\text{I})$ to $d_3a(\text{I})$ band origin can only be explained by explicitly including the bound H(D) atoms in the flipping motion. Consequently, the positions of the internal rotation axes for the flipping monomers within the trimer are crucial. To date, all theoretical models have placed these axes through the bound H(D) atoms, hence excluding their involvement in the vibration. We have demonstrated that by displacing each internal rotation axis so as to allow these bound atoms to move, we are able to qualitatively reproduce the experimental results.

The accuracy of any calculation using a pseudorotation model is dependent on the quality of the torsional PES employed. The two best torsional surfaces in the literature were both calculated assuming the bound H(D) atoms in the trimer remain fixed.^{31,32} Since we have shown this is not the case, neither PES can be expected to reproduce the experimental results accurately. This latter point is not limited to the isotopically substituted trimers but also applies to pseudorotation in the pure trimers. Consequently, the improved understanding of pseudorotation gained from this study should be directly applicable to the pure species. Furthermore, an improved understanding of the dynamics occurring in small water clusters, such as the trimer, should help us to model the spectra of larger clusters. For example, the water pentamer is also predicted to undergo both bifurcation tunneling and pseudorotation, the latter almost certainly offering a route to the assignment of the two pentamer VRT bands observed to date.^{11,12}

Acknowledgment. M.R.V. thankfully acknowledges the Royal Commission for the Exhibition of 1851 for a postdoctoral research fellowship. Funding for this research was provided by the Experimental Physical Chemistry Program of the US National Science Foundation (Grant CHE-9424482).

References and Notes

- (1) Liu, K.; Cruzan, J. D.; Saykally, R. J. *Science* **1996**, *271*, 877.
- (2) Pugliano, N.; Saykally, R. J. *Science* **1992**, *257*, 1937.
- (3) Liu, K.; Loeser, J. G.; Elrod, M. J.; Host, B. C.; Rzepiela, J. A.; Saykally, R. J. *J. Am. Chem. Soc.* **1994**, *116*, 3507.
- (4) Liu, K.; Elrod, M. J.; Loeser, J. G.; Cruzan, J. D.; Pugliano, N.; Brown, M. G.; Rzepiela, J.; Saykally, R. J. *Faraday Discuss.* **1994**, *97*, 35.
- (5) Suzuki, S.; Blake, G. A. *Chem. Phys. Lett.* **1994**, *229*, 499.
- (6) Liu, K.; Brown, M. G.; Viant, M. R.; Cruzan, J. D.; Saykally, R. J. *Mol. Phys.* **1996**, *89*, 1373.
- (7) Cruzan, J. D.; Viant, M. R.; Liu, K.; Brown, M. G.; Saykally, R. J., in preparation.
- (8) Viant, M. R.; Cruzan, J. D.; Brown, M. G.; Saykally, R. J., in preparation.
- (9) Cruzan, J. D.; Braly, L. B.; Liu, K.; Brown, M. G.; Loeser, J. G.; Saykally, R. J. *Science* **1996**, *271*, 59.
- (10) (a) Cruzan, J. D.; Brown, M. G.; Liu, K.; Braly, L. B.; Saykally, R. J. *J. Chem. Phys.* **1996**, *105*, 6634. (b) Cruzan, J. D.; Viant, M. R.; Brown, M. G.; Saykally, R. J. *J. Phys. Chem. A* **1997**, *101*, 9022.
- (11) Liu, K.; Brown, M. G.; Cruzan, J. D.; Saykally, R. J. *Science* **1996**, *271*, 62.
- (12) (a) Liu, K.; Brown, M. G.; Cruzan, J. D.; Saykally, R. J. *J. Phys. Chem. A* **1997**, *101*, 9011. (b) Cruzan, J. D.; Viant, M. R.; Lucas, D. D.; Liu, K.; Brown, M. G.; Saykally, R. J. *J. Phys. Chem.* **1997**, in preparation.
- (13) (a) Liu, K.; Brown, M. G.; Carter, C.; Saykally, R. J.; Gregory, J. K.; Clary, D. C. *Nature* **1996**, *381*, 501. (b) Gregory, J. K.; Clary, D. C.; Liu, K.; Brown, M. G.; Saykally, R. J. *Science* **1997**, *275*, 814. (c) Liu, K.; Brown, M. G.; Saykally, R. J. *J. Phys. Chem. A* **1997**, *101*, 8995.
- (14) Huisken, F.; Kaloudis, M.; Kulcke, A. *J. Chem. Phys.* **1996**, *104*, 17.
- (15) Owicki, J. C.; Shipman, L. L.; Scheraga, H. A. *J. Phys. Chem.* **1975**, *79*, 1794.
- (16) Honegger, E.; Leutwyler, S. *J. Chem. Phys.* **1988**, *88*, 2582.
- (17) Xantheas, S. S.; Dunning, T. H., Jr. *J. Chem. Phys.* **1993**, *98*, 8037.
- (18) Xantheas, S. S.; Dunning, T. H., Jr. *J. Chem. Phys.* **1993**, *99*, 8774.
- (19) Xantheas, S. S. *J. Chem. Phys.* **1995**, *102*, 4505.
- (20) van Duijneveldt-van de Rijdt, J. G. C. M.; van Duijneveldt, F. B. *Chem. Phys.* **1993**, *175*, 271.
- (21) Fowler, J. E.; Schaefer, H. F., III *J. Am. Chem. Soc.* **1995**, *117*, 446.
- (22) Xantheas, S. S. *J. Chem. Phys.* **1994**, *100*, 7523.
- (23) Gregory, J. K.; Clary, D. C. *J. Chem. Phys.* **1995**, *103*, 8924.
- (24) Wales, D. J. *J. Am. Chem. Soc.* **1993**, *115*, 11180.
- (25) Gregory, J. K.; Clary, D. C. *J. Chem. Phys.* **1995**, *102*, 7817.
- (26) Walsh, T. R.; Wales, D. J. *J. Chem. Soc., Faraday Trans.* **1996**, *92*, 2505.
- (27) Schütz, M.; Bürgi, T.; Leutwyler, S.; Bürgi, H. B. *J. Chem. Phys.* **1993**, *99*, 5228.
- (28) Klopper, W.; Schütz, M. *Chem. Phys. Lett.* **1995**, *237*, 536.
- (29) Sabo, D.; Bacic, Z.; Bürgi, T.; Leutwyler, S. *Chem. Phys. Lett.* **1995**, *244*, 283.
- (30) (a) van der Avoird, A.; Olthof, E. H. T.; Wormer, P. E. S. *J. Chem. Phys.* **1996**, *105*, 8034. (b) Olthof, E. H. T.; van der Avoird, A.; Wormer, P. E. S.; Liu, K.; Saykally, R. J. *J. Chem. Phys.* **1996**, *105*, 8051.
- (31) van Duijneveldt-van de Rijdt, J. G. C. M.; van Duijneveldt, F. B. *Chem. Phys. Lett.* **1995**, *237*, 560.
- (32) (a) Bürgi, T.; Graf, S.; Leutwyler, S.; Klopper, W. *J. Chem. Phys.* **1995**, *103*, 1077. (b) Klopper, W.; Schütz, M.; Lüthi, H. P.; Leutwyler, S. *J. Chem. Phys.* **1995**, *103*, 1085.
- (33) Vernon, M. F.; Krajnovich, D. J.; Kwok, H. S.; Lisy, J. M.; Shen, Y. R.; Lee, Y. T. *J. Chem. Phys.* **1982**, *77*, 47.
- (34) Sabo, D.; Bacic, Z.; Graf, S.; Leutwyler, S. *Chem. Phys. Lett.* **1996**, *261*, 318.
- (35) Sorenson, J. M.; Gregory, J. K.; Clary, D. C. *Chem. Phys. Lett.* **1996**, *263*, 680.
- (36) (a) Blake, G. A.; Laughlin, K. B.; Cohen, R. C.; Busarow, K. L.; Gwo, D.-H.; Schmuttenmaer, C. A.; Steyert, D. W.; Saykally, R. J. *Rev. Sci. Instrum.* **1991**, *62*, 1693. (b) Blake, G. A.; Laughlin, K. B.; Cohen, R. C.; Busarow, K. L.; Gwo, D.-H.; Schmuttenmaer, C. A.; Steyert, D. W.; Saykally, R. J. *Rev. Sci. Instrum.* **1991**, *62*, 1701.
- (37) Herriott, D. R.; Kogelnik, H.; Kompfner, R. *Appl. Opt.* **1964**, *3*, 523.
- (38) Liu, K.; Fellers, R. S.; Viant, M. R.; McLaughlin, R. P.; Brown, M. G.; Saykally, R. J. *Rev. Sci. Instrum.* **1996**, *67*, 410.
- (39) Gordy, W.; Cook, R. L. *Microwave Molecular Spectra*, 3rd ed.; Wiley: New York, 1984.
- (40) Lister, D. G.; MacDonald, J. N.; Owen, N. L. *Internal Rotation and Inversion*; Academic Press: London, 1978.